Performance Optimization of Single-Slope Solar Still with Metal Scrap Heat Enhancers via Taguchi Method

(*AI was used in our paper to polish language clarity as well as grammar and sentence structure without involvement in content development or analytical work. All intellectual contributions, research findings, and conclusions are the exclusive work of the authors****)***

Virumandampalayam Perumal Krishnamurthy[1]*, Debabrata Barik[2], Sundararajan Subramanian[3], Naveen Subbaiyan[4]

[1]Research Scholar, Department of Mechanical Engineering, Karpagam Academy of Higher Education, Coimbatore-641021

[2]Department of Mechanical Engineering, Karpagam Academy of Higher Education, Coimbatore-641021, India.

[3]Department of Mechanical Engineering, SCAD College of Engineering and Technology, Tamilnadu, India

[4]Department of Mechanical Engineering, Saveetha School of Engineering, Saveetha Institute of Medical and Technical Sciences, Saveetha University, Chennai, Tamil Nadu, India 602105

*Corresponding author email: vpkkalai2010@gmail.com

Graphical abstract

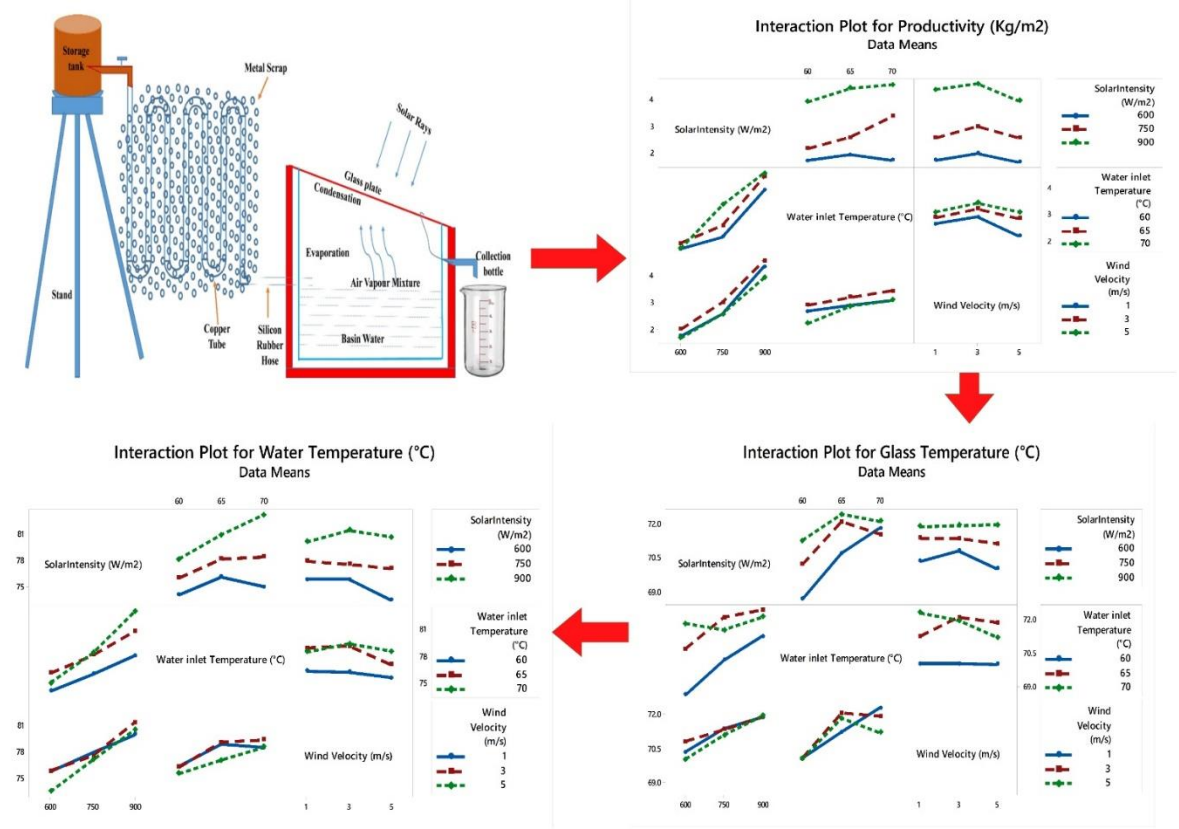

Abstract

This study uses Taguchi analysis to assess the performance and energy efficiency of a metal scrap-incorporating single-slope solar still (SSSS). This study examines the influence of key input variables solar intensity, wind velocity, and water inlet temperature on output metrics such as daily productivity, water temperature, and glass temperature. Experimental trials were conducted with varying input parameters, and the responses were analyzed to determine the optimal conditions for improving system performance. The use of prewarmed saline water, derived from heat energy obtained from metal waste, markedly enhanced the efficiency of the solar still. The findings indicated that the primary factors significantly affecting productivity variations were solar radiation intensity, entering water temperature, and the temperatures of both glass and water. Increased solar intensities of 750 W/m² and 900 W/m², combined with moderate water inlet temperatures of 70°C, enhanced productivity, reaching a maximum of 4.71 kg/m² under optimal conditions. Wind velocity exerted a cooling influence, diminishing system efficiency at elevated speeds, whereas moderate wind levels of 3 m/s enhanced overall heat transfer. The Two-Way Normal ANOM, contour plots, and main effects plots illustrated the synergistic effects of input parameters on system performance, underscoring the significance of parameter optimization. The research shows that solar stills may be much more efficient when they use thermal energy from metal waste and when they fine-tune operational variables. In areas where freshwater is in short supply, this study suggests a way to improve solar still designs, which might help in the hunt for long-term water purification options.

Keywords: Single slope solar still, metal scrap, Taguchi Method, productivity, Water Temperature, Glass Temperature.

1. Introduction

The world faces numerous challenges, including overpopulation and critical issues that threaten sustainability. A key contributor to the problem of climate change is the increased carbon dioxide production from burning fossil fuels [1]. Reliable access to energy and water is essential for improving quality of life, facilitating diverse human activities, and advancing social progress. Solar energy has emerged as a sustainable solution for desalination, offering a renewable energy alternative with considerable

potential. Desalination represents a viable method within renewable energy technologies, particularly when combined with solar distillation [2]. Providing clean drinking water and satisfying resource needs continue to pose considerable challenges in various global regions [3]. Solar distillation is considered an efficient desalination technology, characterized by its simple operation and design [4]. Phase change materials (PCMs) are employed in diverse applications owing to their distinctive thermal characteristics, which include phase change temperatures, thermal conductivity, and latent heat storage capacities. Each phase change material (PCM) has specific advantages and disadvantages relevant to its application, requiring careful selection. Renewable energy applications heavily rely on thermal energy storage (TES) technologies, which can store significant amounts of energy while ensuring stable temperature maintenance. Latent energy storage exhibits a greater energy retention capacity than sensible heat storage, thereby improving the efficiency of traditional solar stills (TSS) [5,6]. The charging phase absorbs heat, while the discharge phase releases it when integrated with phase transition materials. During phase transitions, substances maintain sensible heat at elevated temperatures and latent heat below their melting point [7], [8], [9]. Researchers have examined several thermal energy storage materials to make solar distillation systems more efficient. According to studies on heat efficiency, covered sponges and black igneous rocks are in the rear, with untreated sponges doing best [10]. Significant gains in water production, from 5.1 kg/m²/day to 6.7 kg/m²/day, have been achieved by introducing phase change materials (PCMs) in weir-type cascade solar stills [11]. Additional research has investigated the impact of paraffin wax-filled circular pipe absorbers, enhancing collector efficiency from 45% to 50% [12]. The combination of petroleum jelly and aluminum tubes as phase change materials has improved performance relative to alternative materials [13].

Geometry plays a crucial role in thermal energy storage (TES) systems, as spherical shapes demonstrate superior capacity for storing and releasing thermal energy compared to cylinders, plates, and tubes [14]. Nanomaterials improve the solidification processes, melting points, latent heat, and conductivity of phase change materials (PCMs). Investigations into solar distillation incorporating phase change materials and nanoparticles remain nascent; however, this integration notably decreases the durations of freezing and melting cycles, enhancing heat transfer efficiency [15], [16].

Research conducted by Sonker et al. [17] suggests that nCuO nanoparticles added to paraffin wax have the potential to boost distillate yields by 94.19 percent. A 70.5% improvement in thermal conductivity and a decrease in solidification and melting durations are seen when paraffin and stearic acid nanoparticles are mixed [18], [19]. Research on copper nanocomposites combined with paraffin wax has underscored their potential to enhance thermal conductivity [20]. The results highlight the need to evaluate phase change material melting and solidification characteristics in combination with nanoparticle integration to improve solar still system efficiency [21], [22].

Despite extensive research on heat exchangers and phase change materials in solar desalination systems, several gaps remain unaddressed. While studies have focused on the benefits of conventional and PCM-based heat exchangers, no work has been done on using metal scrap heat exchangers for preheating feed water. The research focuses on enhancing the productivity of the solar still by preheating the water through the copper metal scrap heat exchanger. The copper metal scrap is used outside the solar still to preheat water so it does not have direct contact with the saline water. The Taguchi method is used to optimize the process parameters. The input parameters, which include solar intensity, water inlet temperature, wind velocity, and the corresponding output response, are productivity, glass temperature, and water temperature and are investigated in this research.

2. Taguchi Analysis

Taguchi analysis is a commonly employed technique for designing and executing experiments to evaluate the impact of various factors on a process, thus avoiding the need to test every potential variable combination, which can be both time-intensive and expensive [23]. The Taguchi methodology aids in identifying the preferred design by choosing the configuration that attains optimal performance under defined conditions. Applying orthogonal arrays in designing systems like solar stills provides significant advantages, including simplicity and adaptability [24, 25]. This method is advantageous for intricate experiments encompassing various factors and levels, as it facilitates extracting essential information with fewer trials. The Taguchi method analyzes the influence of noise on process output through the computation of the signal-to-noise (S/N) ratio, which is utilized for performance evaluation. An

examination of the signal-to-noise ratio reveals the proximity of the average response to the target values and the extent of variance present in the data. Calculating the signal-to-noise ratio is crucial for assessing experimental data, as it is contingent upon the particular quality attributes of the factors involved. Wang et al. [26] performed experiments utilizing Taguchi analysis and analysis of variance to examine the effects of various variables on solar still production. Research demonstrates that the temperature of salt water significantly affects the system's efficacy. Samara et al. [27] examined the influence of glass cover angle and saltwater temperature on the efficiency of solar stills, finding that both factors significantly enhanced performance. Ali et al. [28] improve the design of the single-slope solar still through Taguchi analysis. Their findings indicate that salt water and glass enhance system performance. The Taguchi method divides signal-to-noise (S/N) ratios into three classes based on a quality metric: (i) more minor is better, (ii) nominal is best, and (iii) greater is better [29]. The S/N ratios, namely "larger is better" (LB), "smaller is better" (SB), and "nominal is best" (NB), are computed using specific equations designed for the quality characteristics of the experimental system.

S/N ratio for SB=$10log_{10}\left[\sum\frac{Y^2}{n}\right]$..... (1)

S/N ratio for NB=$10log_{10}\left[\frac{Y}{S^2}\right]$..... (2)

S/N ratio for LB=$10log_{10}\left[\frac{1}{n}\sum\frac{1}{Y^2}\right]$..... (3)

Here, 'Y' stands for the response, 'n' for the total number of responses, and for the variance of the observed data overall aspect combinations. According to the reviewed literature, solar stills have been known to use various sensible heat storage materials to increase their efficiency. Metal scrap as a sensible heat storage medium in solar stills has not been the subject of enough experimental study, and the Taguchi technique for optimizing performance parameters has not been investigated either. Discovering the key performance indicators impacting distillate yield, this research evaluates the effectiveness of a solar still. This approach also acknowledges the importance of sun intensity, water inlet temperature, and wind velocity as significant performance parameters. To improve the efficiency and effectiveness of solar desalination systems, this study seeks to maximize their productivity by using the Taguchi approach.

3. Experimental Setup

3.1. Single slope solar still

The schematic of an SSSS is shown in Figure 1. The layout reflects the usual components of a solar still system and includes the storage tank, thermometers, pipe network, and solar still. In conjunction with the piping and thermometry setup, the storage tank and solar still are essential components [30]. The solar still basin is constructed from galvanized iron with a thickness of 2 mm and a depth of 0.12 m. The entire surface of the basin is matte black to optimize solar absorption. The basin is contained within a wooden box measuring 1.2 m by 1.2 m, with a thickness of 0.19 m and a height of 0.1 m. The interior of the wooden box is painted white to enhance sunlight penetration to the water's surface, following the filling of the basin with sawdust and its placement between the wooden enclosure to minimize heat loss [31]. The experimental setup was constructed and tested at Erode, located at 11.3410° N and 77.7172° E. The hardwood box was topped with a 5 mm thick glass pane tilted at an 11° angle. Sheet metal covered all five sides of the wooden container, shielding the setup from the elements.

A single-slope solar still, an effective and affordable way to purify water using solar energy, is shown in Figure 1. The configuration comprises a storage tank that contains raw or impure water, which is directed into the still via a water inlet to ensure a stable water level. The inclined glass covers facilitate sunlight entry, warming the water and creating a greenhouse effect that promotes evaporation. Water vapor ascends and undergoes condensation on the cooler inner surface of the glass, resulting in droplets descending due to the slope. The purified water, free from impurities, is collected through a distillate outlet and stored in a measuring jar for quantification. This passive system utilizes solar energy exclusively, rendering it an environmentally sustainable and effective method for delivering clean water in resource-constrained regions.

.

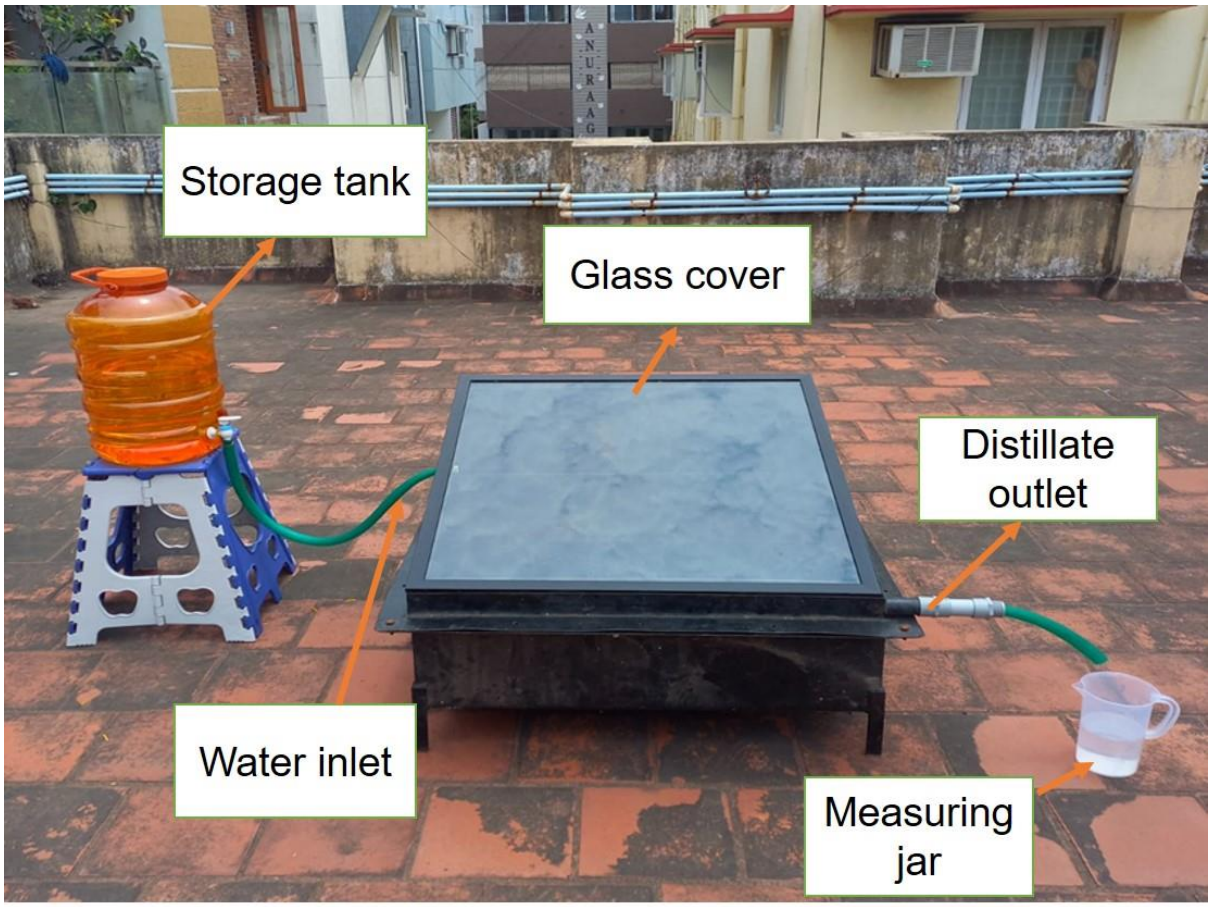

Figure 1 Single Slope Solar Still

3.2. Single-Slope Solar Still with Metal Scrap Heat Enhancers

This research examines solar intensity, water inlet temperature, and wind velocity as critical factors affecting the efficiency of an SSSS enhanced by metal scrap heat exchangers. The selection and arrangement of metal scrap significantly influence the thermal efficiency of an SSSS. Metals such as aluminium, copper, and steel demonstrate differing thermal conductivities, directly affecting their ability to absorb, store, and transfer heat. This research utilized copper scrap as a heat exchanger due to its enhanced thermal conductivity relative to alternative metals, facilitating efficient heat transfer and augmenting evaporation rates. This research employed copper scrap fragments ranging from 10 mm to 30 mm long and 3 mm to 8 mm thick. The size selection optimizes the equilibrium between surface area for heat transfer and thermal storage capacity. Smaller pieces offer increased surface area, facilitating quicker heat absorption, whereas larger pieces enhance prolonged thermal energy retention. Due

to forming a protective coating of cuprous oxide (CuO), which lessens the possibility of further oxidation, copper metal scrap has exceptional corrosion resistance. Cuprous chloride (CuCl), which may cause localized pitting corrosion under extreme circumstances, can occur in saline settings after prolonged contact with chloride ions. Unlike ferrous metals, which undergo continuous oxidation, copper exhibits self-limiting corrosion, making it a more robust and reliable material for protracted usage in solar stills. Particularly in areas with high salinity and humidity, the longevity and effectiveness of copper scrap as a heat-enhancing material in solar desalination systems can be increased by putting protective measures like surface passivation, polymer coatings, and routine maintenance into practice.

Figure 2 shows the SSSS with metal scrap heat exchangers. An elevated storage tank provides the raw water for the system, which is then heated by solar radiation passing through an angled glass plate. The water is sent to the basin via a flow control valve. The condensation of vapor on the glass surface, induced by the greenhouse effect, facilitates accelerated water evaporation, ultimately leading to its collection in a bottle positioned below. To improve performance, the system integrates a metal scrap heat exchanger linked through a silicon rubber hose and copper tubing. Radiation, convection, and conduction influence the improvement of heat transfer in solar still utilizing scrap copper metal. Conduction occurs when copper's strong thermal conductivity efficiently absorbs sunlight and transmits heat to nearby water, increasing evaporation. Because the heated metal scrap produces localized temperature gradients, convection is improved. These gradients provide natural convective currents, which promote heat circulation and lessen thermal stratification. By allowing copper surfaces to absorb and re-emit heat energy, radiation helps to keep water temperatures high even when the sun's intensity fluctuates. When these heat transfer processes work together, the solar thermal efficiency increases, leading to higher evaporation rates and more freshwater output. The copper metal scrap preheats the saline water before entering the solar still. Preheated water necessitates reduced heat energy for evaporation within the solar still. Metal scrap improves heat transfer to water by storing and radiating additional thermal energy, facilitating evaporation. A method for producing clean water that is both efficient and cost-effective is realized through the integration of passive solar heating and active thermal augmentation, resulting in enhanced distillate output.

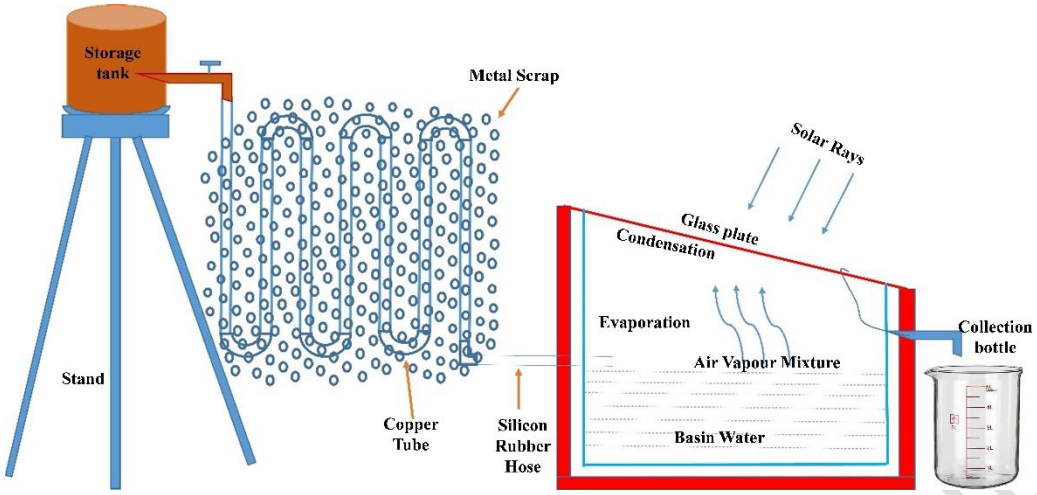

Figure 2. SSSS with metal scrap Heat Enhancers

Table 1 illustrates how the system's operational efficiency impacts the wind speed, intake water temperature, and solar intensity. The L_{27} OA produced using Taguchi's design methodology is displayed in Table 2.

Table 1 Input parameters and their levels

Sl. No	Parameters	Notation	Levels		
			-1	0	+1
1	Solar intensity (W/m^2)	SI	600	750	900
2	Water inlet temperature (°C)	WI	60	65	70
3	Wind Velocity(m/s)	WV	1	3	5

Table 2 Taguchi L_{27} array design

S.No	SI (W/m^2)	WI (°C)	WV (m/s)
1	600	60	1
2	600	60	3
3	600	60	5
4	600	65	1
5	600	65	3
6	600	65	5
7	600	70	1
8	600	70	3

9	600	70	5
10	750	60	1
11	750	60	3
12	750	60	5
13	750	65	1
14	750	65	3
15	750	65	5
16	750	70	1
17	750	70	3
18	750	70	5
19	900	60	1
20	900	60	3
21	900	60	5
22	900	65	1
23	900	65	3
24	900	65	5
25	900	70	1
26	900	70	3
27	900	70	5

4. Analysis of Variance (ANOVA)

Analyzing the link between categorical and response variables is essential for many kinds of research, and Analysis of Variance (ANOVA) is a potent tool for this purpose. Using categorical categories and other sources of variation, the ANOVA statistical approach divides the total variance of a response variable into its component components. The mean of different groups or levels within a factor may then be compared to see whether there is a statistically significant difference [32]. ANOVA allows us to systematically ascertain the impact of each geometrical parameter on the answer variable. This approach focuses on how factor-level differences produce variability across groups instead of the variability within groups that arises from random or unexplained variance. A significant influence of the geometric parameter on the answer is shown by the fact that there is far more variation across groups than within them. This analysis provides critical insights into the importance of each factor

and assists in identifying the parameters that significantly affect variations in the response variable.

5. Results and Discussion

The criteria used to assess the system's performance in this research include solar intensity (SI) ranging from 600 to 900 W/m², water inlet temperature (WI) from 60 to 70°C, and wind velocity (WV) from 1 to 5 m/s. Key performance indicators are water temperature (T_w) and glass temperature (T_g), both expressed in degrees Celsius, and system productivity (P) measured in kg/m². Increases in SI, when combined with targeted values of WI and WV, significantly boost output. At 900 W/m² of solar irradiation (SI), 70°C of water intake temperature (WI), and 3 m/s of wind velocity (WV), peak productivity (P) was achieved. Even though the experimental settings were varied, the water temperature (T_w) was steady throughout, staying within a range of 72 to 80°C. The experimental data examined using the Taguchi Method are shown in Table 3.

Table 3. Experiment values of solar desalination with the use of metal scrap for preheating observations by Taguchi method

S.No	SI (W/m^2)	WI (°C)	WV (m/s)	P (g/m^2)	T_w (°C)	T_g(°C)
1	600	60	1	1.76	74.81	68.54
2	600	60	3	1.98	75.23	69.94
3	600	60	5	1.38	72.11	67.54
4	600	65	1	1.93	76.4	71.22
5	600	65	3	2.01	77.56	70.26
6	600	65	5	1.84	74.36	70.59
7	600	70	1	1.48	76.22	71.29
8	600	70	3	1.96	74.71	72.26
9	600	70	5	1.74	73.98	71.94
10	750	60	1	2.01	77.13	70.42
11	750	60	3	2.34	74.35	68.99
12	750	60	5	2.11	76.58	71.23
13	750	65	1	2.35	79.48	71.25

14	750	65	3	2.98	78.79	73.48
15	750	65	5	2.43	76.28	71.54
16	750	70	1	3.31	77.18	72.46
17	750	70	3	3.64	79.52	71.62
18	750	70	5	3.12	78.46	70.57
19	900	60	1	4.21	77.05	71.21
20	900	60	3	4.39	79.18	71.24
21	900	60	5	3.11	78.01	71.32
22	900	65	1	4.36	80.96	71.28
23	900	65	3	4.63	81.11	72.54
24	900	65	5	4.28	80.56	73.45
25	900	70	1	4.49	82.17	73.21
26	900	70	3	4.71	84.01	72.01
27	900	70	5	4.42	83.24	71.14

5.1 Effect of SSS variables for Main Effects Plots for Means and S/N ratio.

Figure 3 shows the "Main Effects Plot for Means," which shows how Solar Intensity (SI), Water input temperature (WI), and Wind Velocity (WV) affect performance in the system. Solar intensity shows an apparent positive effect, with productivity increasing steadily as SI rises from 600 to 900 W/m², indicating its significant role in enhancing performance. Productivity improves when WI climbs from 60°C to 70°C, suggesting a positive trend in water intake temperature. This improvement is likely attributable to improved thermal efficiency. The velocity of wind has a substantial effect on the productivity of SSSS through its influence on heat transfer processes. Moderate wind velocity, approximately 3 m/s, facilitates evaporation by diminishing the thickness of the thermal boundary layer, which in turn enhances heat transfer and promotes increased water vapor generation. Excessive wind velocity (5 m/s) increases convective heat losses from the water surface and the glass cover, diminishing the temperature gradient required for effective condensation and overall distillate yield. Controlled airflow enhances system performance by sustaining optimal thermal conditions; however, excessive cooling disrupts energy balance, decreasing productivity [33]. The parameters with the most noticeable effects are SI and WI, but WV's effect is non-linear [34, 35].

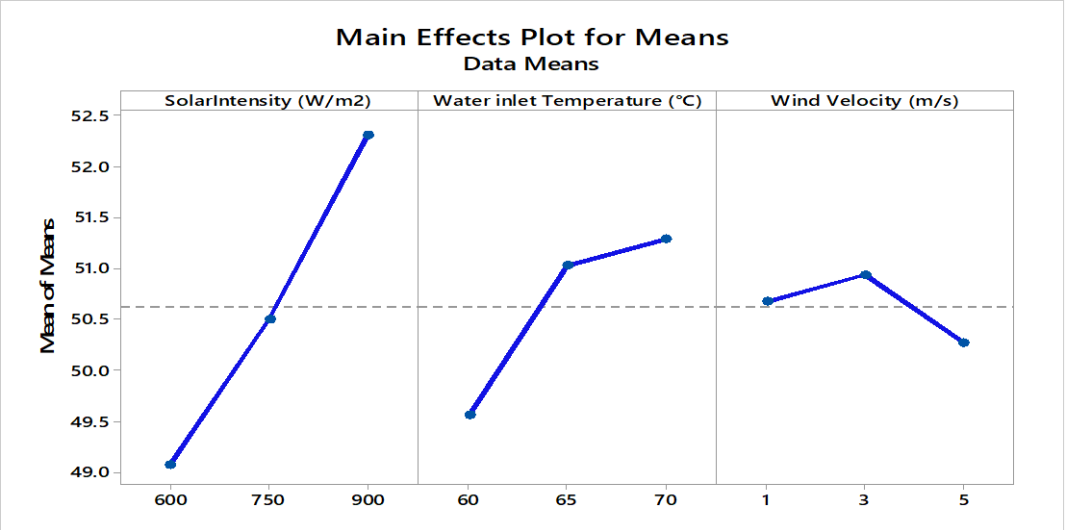

Figure 3. Main Effects Plot for Means in Taguchi Optimization Process.

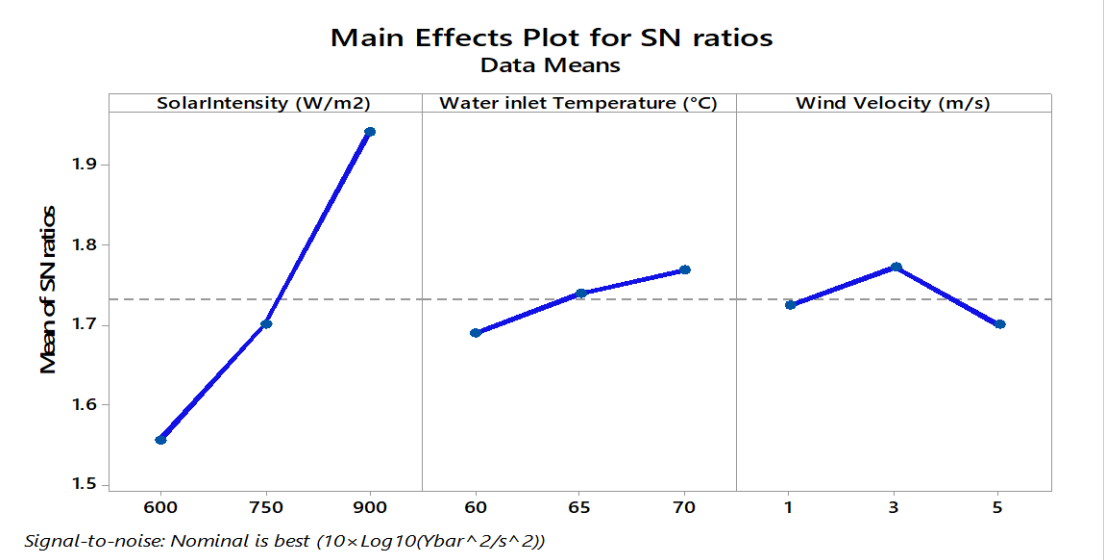

Figure 4. Main Effects Plot for Means of S/N ratios Taguchi Optimization Process.

Solar Intensity (SI), Water Inlet Temperature (WI), and Wind Velocity (WV) are shown in the "Main Effects Plot for SN Ratios" to show how they affect the stability and productivity of the system's performance. Solar Intensity demonstrates a substantial positive effect, as the SN ratio consistently increases with SI ranging from 600 to 900 W/m², signifying improved productivity and diminished variability. As the temperature rises from 60°C to 70°C, the signal-to-noise ratio somewhat improves, indicating better thermal efficiency, and the water intake temperature exhibits a favorable trend. The

signal-to-noise ratio improves at moderate airflow (3 m/s) but decreases at higher speeds (5 m/s), likely due to disturbed thermal stability; this non-linear influence of wind velocity is seen. Optimizing these parameters, especially SI and moderate WV, enhances productivity and system consistency, as shown in Figure 4.

Table 4. Response Table for Signal to Noise Ratios for P

Level	SI (W/m^2)	WI (°C)	WV (m/s)
1	1.556	1.689	1.725
2	1.700	1.740	1.773
3	1.942	1.769	1.700
Delta	0.386	0.080	0.073
Rank	1	2	3

Table 5. Response Table for Means for P

Level	SI (W/m^2)	WI (°C)	WV (m/s)
1	49.08	49.56	50.67
2	50.50	51.03	50.94
3	52.31	51.29	50.27
Delta	3.23	1.73	0.67
Rank	1	2	3

Table 6. Analysis of Variance for P

Source	DF	Adj SS	Adj MS	F-Value	P-Value
SI (W/m^2)	2	28.864	14.4320	141.38	0.000
WI (°C)	2	1.769	0.8846	8.67	0.002
WV (m/s)	2	1.015	0.5073	4.97	0.018

Error	20	2.042	0.1021		
Total	26	33.689			

Regression Equation

Productivity (kg/m^2) = 2.9248 - 1.1381 Solar Intensity (W/m2)_600 - 0.2259 Solar Intensity (W/m^2)_750 + 1.3641 Solar Intensity (W/m^2)_900- 0.3370 Water inlet Temperature (°C)_60 + 0.0541 Water inlet Temperature (°C)_65+ 0.2830 Water inlet Temperature (°C)_70- 0.0470 Wind Velocity (m/s)_1+ 0.2574 Wind Velocity (m/s)_3 - 0.2104 Wind Velocity (m/s)_5

Table 7. Analysis of Variance for T_w

Source	DF	Adj SS	Adj MS	F-Value	P-Value
SI (W/m^2)	2	144.686	72.343	37.57	0.000
WI (°C)	2	40.223	20.112	10.44	0.001
WV (m/s)	2	6.996	3.498	1.82	0.188
Error	20	38.510	1.925		
Total	26	230.415			

Regression Equation

Water Temperature (°C) = 77.757 - 2.715 Solar Intensity (W/m2)_600 - 0.227 Solar Intensity (W/m^2)_750 + 2.942 Solar Intensity (W/m^2)_900 - 1.707 Water inlet Temperature (°C)_60 + 0.632 Water inlet Temperature (°C)_65 + 1.075 Water inlet Temperature (°C)_70 + 0.176 Wind Velocity (m/s)_1 + 0.516 Wind Velocity (m/s)_3 - 0.693 Wind Velocity (m/s)_5

Table 8. Analysis of Variance for T_g

Source	DF	Adj SS	Adj MS	F-Value	P-Value
SI (W/m^2)	2	10.6955	5.3477	5.29	0.014
WI (°C)	2	18.1285	9.0642	8.97	0.002
WV (m/s)	2	0.5069	0.2534	0.25	0.041
Error	20	20.2138	1.0107		
Total	26	49.5447			

Regression Equation

Glass Temperature (°C) = 71.205 - 0.807 Solar Intensity (W/m2)_600
+ 0.079 Solar Intensity (W/m2)_750 + 0.728 Solar Intensity (W/m2)_900
- 1.157 Water inlet Temperature (°C)_60
+ 0.529 Water inlet Temperature (°C)_65
+ 0.628 Water inlet Temperature (°C)_70
+ 0.004 Wind Velocity (m/s)_1
+ 0.166 Wind Velocity (m/s)_3
- 0.170 Wind Velocity (m/s)_5

Forecasting, risk assessment, and optimization of systems are among some of the numerous practical applications of regression models. Within the restrictions of the inputs given for model development, these models can predict and offer understanding of the system's behavior by establishing links between the dependent and independent variables. Estimates of potential outcomes are based on the R2 (regression coefficient) value found when equations are developed. When optimizing a system, regression models are useful for making better decisions, optimizing performance using empirical data, and fine-tuning parameters.For example, a manufacturer aims to reduce production costs while enhancing output through the application of a regression equation: Cost = 500 + 20 (units produced) - 0.05 (units produced^2). Taking the derivative and setting it to zero yields the equation 20 - 0.1(Units Produced) = 0, which indicates that the optimal production level is 200 units.

This facilitates the equilibrium between cost efficiency and production output, thereby maximizing profitability.

Table 4 presents a ranking of the effects of Solar Intensity (SI), Water Inlet Temperature (WI), and Wind Velocity (WV) on the signal-to-noise (SN) ratio for productivity (P). SI exhibits the most significant impact, with the largest delta of 0.386, followed by WI at 0.080 and WV at 0.073, highlighting its significant role in stabilizing system performance. Table 5 assesses the average productivity across various factor levels. SI demonstrates the most substantial effect, with productivity rising markedly from 49.08 kg/m² at 600 W/m² to 52.31 kg/m² at 900 W/m².Table 6 presents the ANOVA results for P, indicating that SI is the most significant factor (F-value = 141.38, P = 0.000), followed by WI (F = 8.67) and WV (F = 4.97). All factors significantly affect productivity, with SI accounting for the most significant variability. The regression equation for P indicates positive contributions from elevated solar irradiance (900 W/m²) and water temperature (70°C), while the impact of wind velocity is minimal, with moderate speeds (3 m/s) being optimal [36]. Table 7 presents the ANOVA results for T_w, indicating that SI and WI have significant effects on water temperature (F = 37.57 and 10.44, respectively), whereas WV demonstrates a negligible impact (P = 0.188). The regression equation for T_w indicates that elevated levels of SI and WI have a positive effect on T_w, thereby sustaining stable thermal conditions. Table 8 presents the ANOVA results for T_g, indicating that WI is the most significant factor influencing glass temperature (F = 8.97, P = 0.002), with SI following (F = 5.29). WV demonstrates a minimal but significant effect (P = 0.041). The regression equation for T_g indicates that higher WI and SI contribute positively, while WV has a minimal effect. SI is the primary contributor across all outputs, followed by WI, while WV has the least influence [37].

5.2 Effect of SSS variables on P, T_w, and T_g.

Solar intensity, water input temperature, and wind velocity affect the system's performance. The effect of input process parameters on productivity (P) is shown in Figure 5. The solar intensity significantly influences solar still productivity, rising from 1.8 Kg/m² at 600 W/m² to 4.5 Kg/m² at 900 W/m², as increased thermal energy input enhances evaporation. The temperature of the water inlet has a positive effect on productivity, increasing from 2.6 Kg/m² at 60°C to 3.3 Kg/m² at 70°C, as preheated water necessitates less supplementary energy for phase change. Wind velocity

demonstrates a non-linear relationship with productivity, as moderate wind speed (3 m/s) enhances output from 2.9 Kg/m² to 3.2 Kg/m² by optimizing convective heat transfer. Conversely, high wind speed (5 m/s) leads to a decline in productivity to 2.7 Kg/m², attributed to heightened convective heat loss. Consequently, although solar intensity is the primary factor, optimizing water temperature and wind velocity is essential to enhance distillate yield.

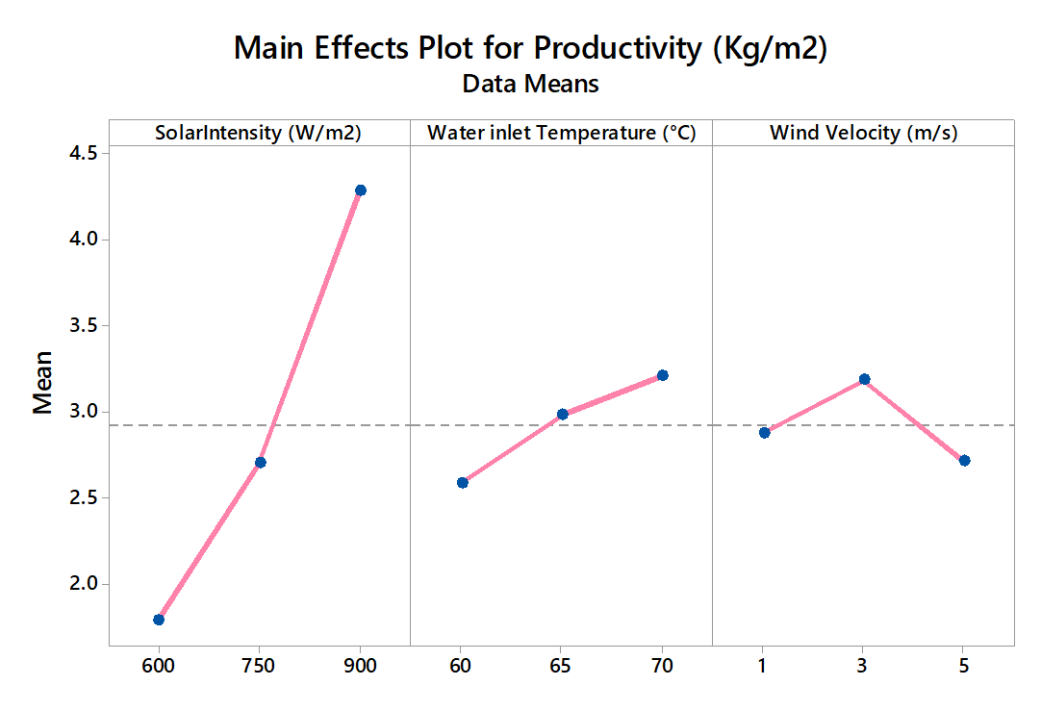

Figure 5. Main Effects plot for P in Taguchi Analysis

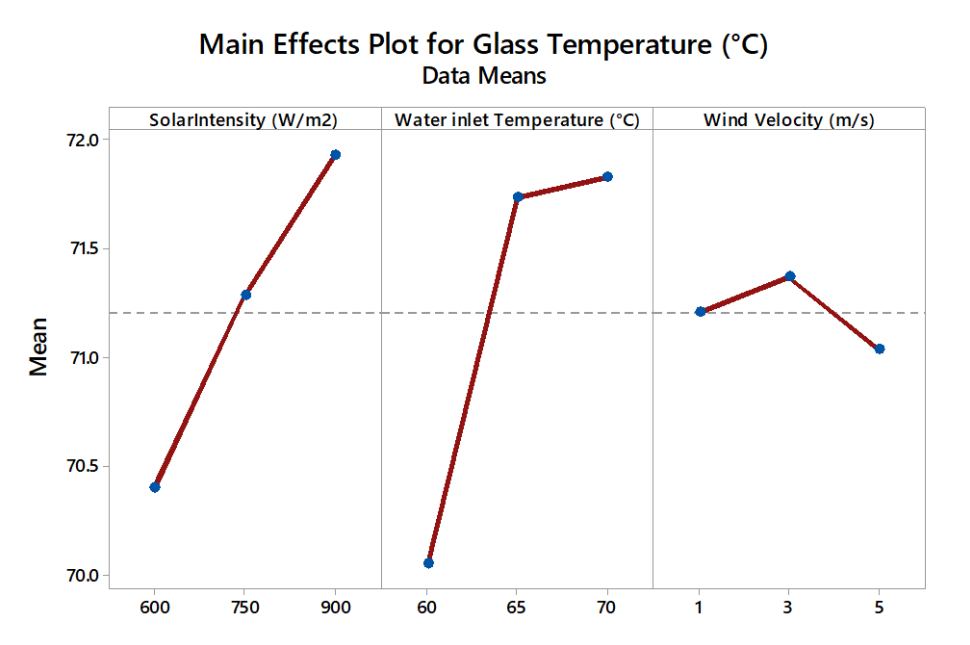

Figure 6. Main Effects plot for T_g in Taguchi Analysis.

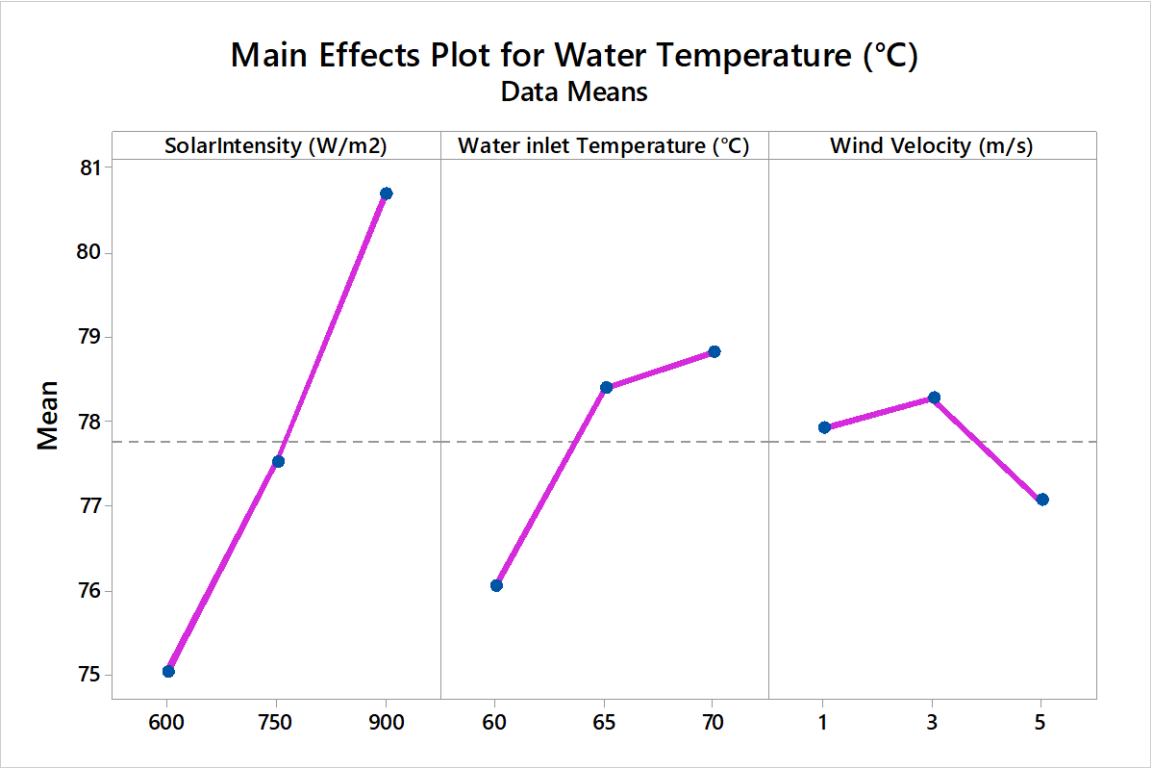

Figure 7. Main Effects plot for T_W in Taguchi Analysis

Figure 6 shows the influence of input process parameters on T_g. It indicates a significant increase in glass temperature with rising solar intensity, escalating from 70.2°C at 600 W/m² to 72.0°C at 900 W/m², attributed to enhanced radiation absorption. The temperature of the water inlet influences the glass temperature, rising from 70.0°C at 60°C to 71.8°C at 70°C, as elevated water temperatures diminish heat loss to the glass. Wind velocity follows a non-linear trend. At 3 m/s, it maximizes glass temperature (71.3°C), but at 5 m/s, it drops to 71.0°C due to increased convective [38, 39]. The main effect plots of Tw are shown in Figure 7. The main effects plot shows that water temperature increases significantly with solar intensity, rising from 75.0°C at 600 W/m² to 81.0°C at 900 W/m², due to higher heat absorption. The temperature of the water inlet positively affects the overall water temperature, rising from 76.0°C at 60°C to 79.0°C at 70°C, as preheated water diminishes initial heating demands. At 3 m/s, it maximise the water temperature (78.5°C) but at 5 m/s, it drops to 77.0°C due to greater convective heat losses. Solar intensity exerts the most substantial influence, succeeded by water inlet temperature, whereas moderate wind speeds contribute to maintaining elevated water temperatures.

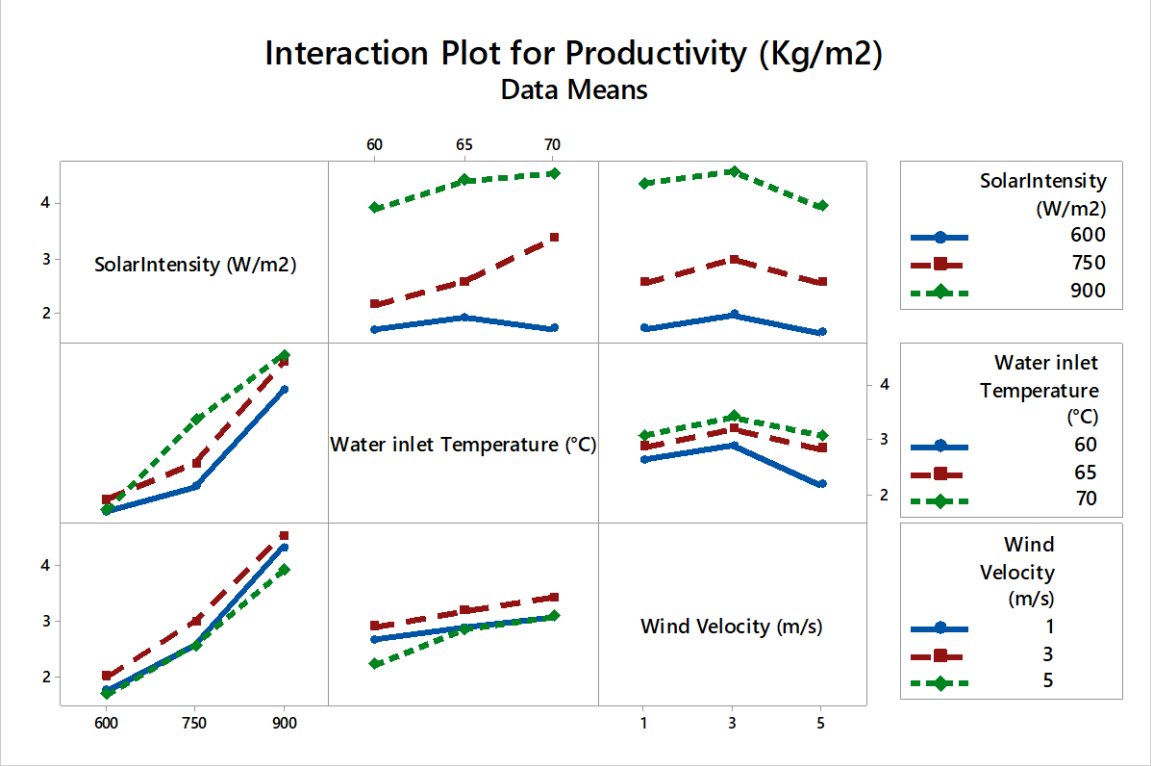

Figure 8. Interaction Plot for P in Taguchi Analysis

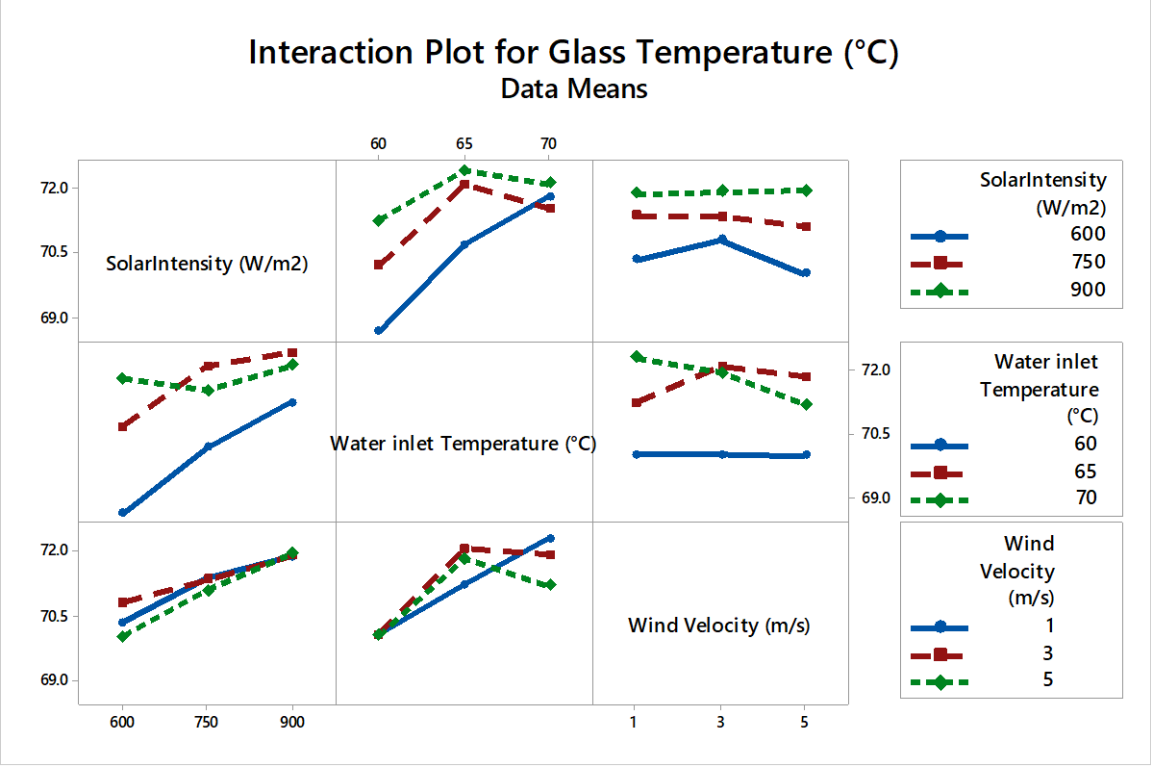

Figure 9. Interaction Plot for T_g in Taguchi Analysis

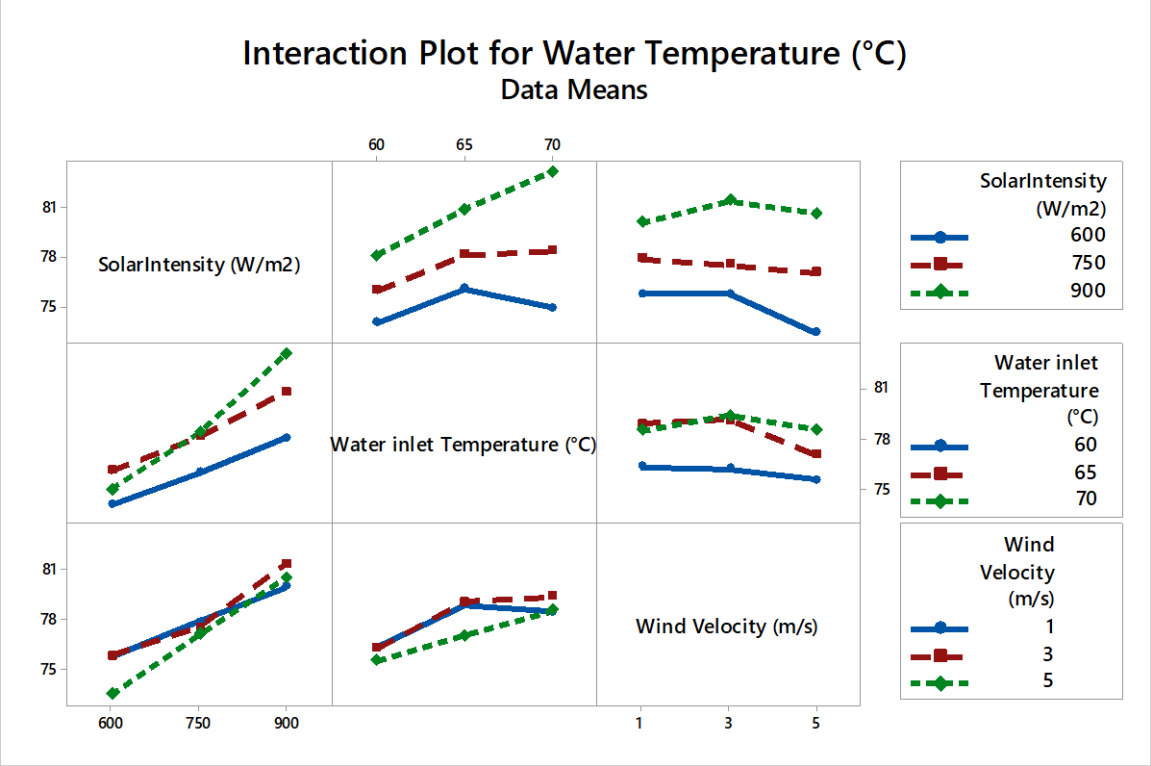

Figure 10. Interaction Plot for T_w in Taguchi Analysis

This interaction plot visualizes the collective influence of input factors on the resulting output. If parallel lines represent the relationship, there is no influence from combining one factor with another. Conversely, non-parallel lines indicate a significant interaction effect in the relationship [40,41]. Figures 8, 9, and 10 illustrate the interaction among the considered inputs over productivity (P), glass temperature (T_g), and water temperature (T_w), respectively.

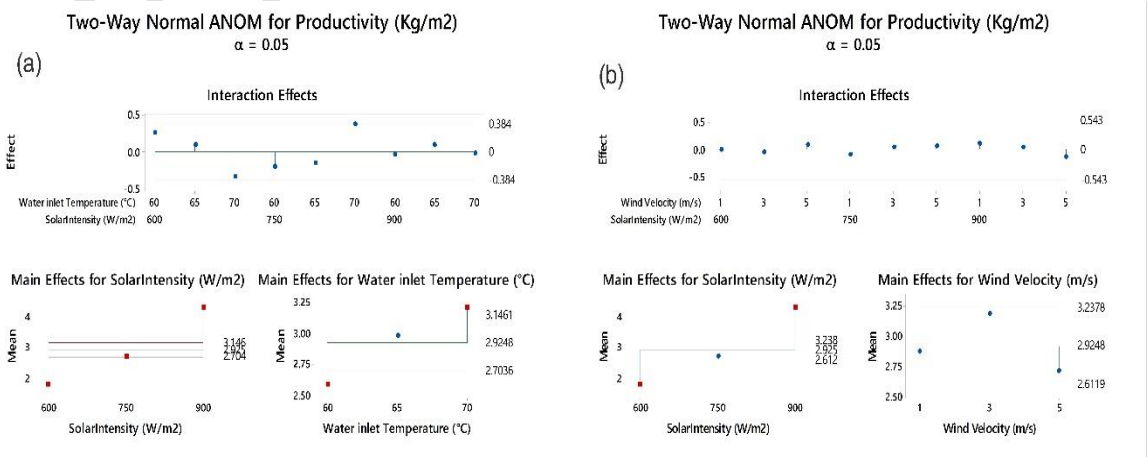

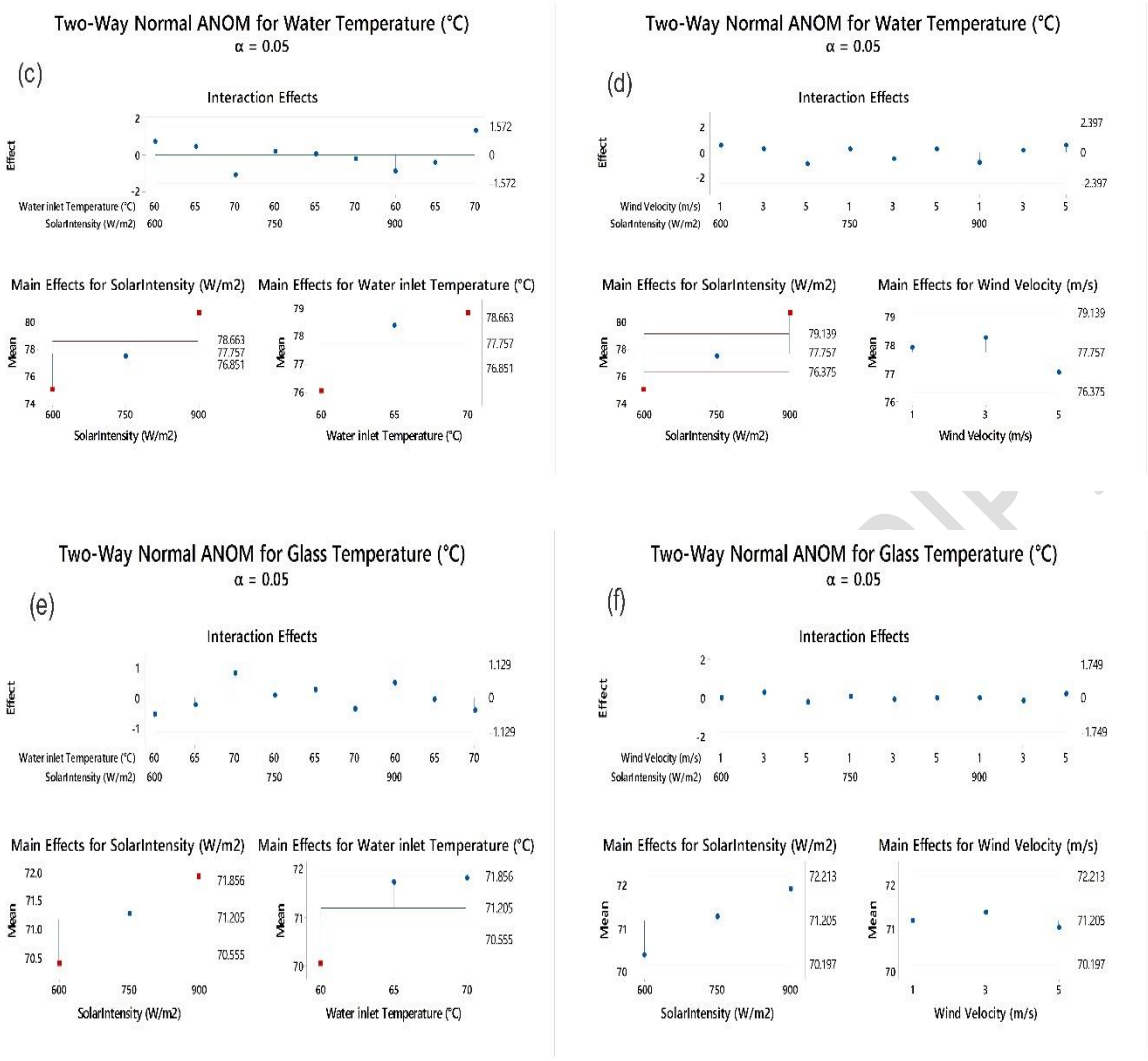

Figure 11. Two way Normal ANOM for Output Responses

The combined impacts of variables, including wind velocity (e, f), water inlet temperature (c, d), and sun intensity (a, b) on output responses are evaluated using the two-way normal ANOM, which is shown in Figure 11. According to the data table, higher sun intensity (750 W/m² and 900 W/m²) often exhibits positive deviations, leading to higher temperatures and production. The greatest productivity is 4.71 kg/m² when the irradiance is 900 W/m². Performance is somewhat reduced at high temperatures, while best results are obtained at moderate intake temperatures of 65°C. Wind velocity hurts responses; responses are better at 1 m/s and 3 m/s than at 5 m/s. Productivity is 4.49 kg/m² at 900 W/m² intensity and 1 m/s velocity but drops to 4.42 kg/m² as velocity rises to 5 m/s. The ANOM indicates that optimal performance is achieved by combining high solar intensity, moderate inlet temperature, and low wind velocity, consistent with the trends presented in Table 3. Negative deviations

manifest at elevated wind velocities and extreme temperatures, signifying regions of inefficiency.

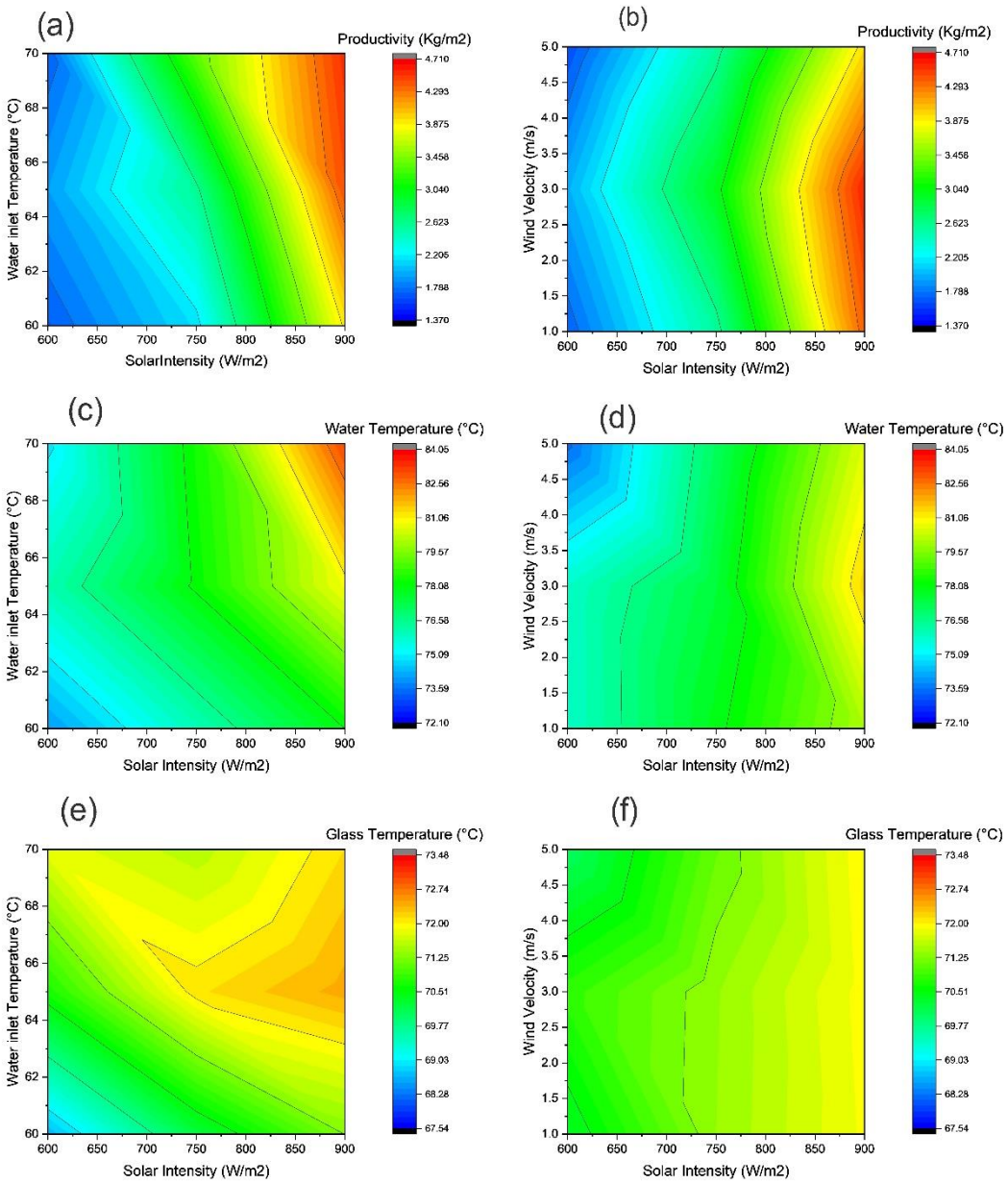

Figure 12. Contour Plots for Output Responses of Taguchi Analysis

Figure 12 illustrates contour plots that depict the combined effects of two factors on output responses, including productivity (P) (a, b), glass temperature (T_g) (c, d), and water temperature (T_w) (e, f). As the data table indicates, increased solar intensity (750 W/m² and 900 W/m²) consistently results in improved output responses. Productivity reaches 4.71 kg/m² at 900 W/m² of irradiance and 65°C, maintaining the contour plot's trend [42]. Across a range of sun intensities, moderate water inlet temperatures of

65°C provide the best outcomes. The water and glass temperatures reach a maximum of 84.01°C with an intensity of 900 W/m². The contour plots visually represent these values, with a steep gradient signifying increased productivity and temperature. While not explicitly described in the contour plots, wind velocity negatively influences output responses. The data table indicates that increased wind speeds (5 m/s) are associated with decreased productivity and temperatures. The contour plots indicate optimal conditions at moderate inlet temperatures and elevated solar intensity, corroborating the observed data trends. The plots illustrate the interaction between these factors and their influence on system performance [43].

6. Economic Feasibility Study of Heat Enhancement Methods

Table 9 presents the economic feasibility analysis of heat enhancement methods. The payback period is determined by dividing the fabrication cost by the net profit, which represents the difference between water production costs and maintenance expenses. The findings indicate that metal scrap presents the highest economic viability, characterized by the fastest return on investment and the lowest overall costs, thereby establishing it as the most sustainable and economically favorable method for heat enhancement.

Table 9 Economic Feasibility Study of Heat Enhancement Methods

S.No	Heat Enhancement Method	Material Cost (Rs)	Maintenance per Day (Rs)	Purified water cost (Rs)	Net profit Per day (Rs)	Payback Period (Days)
1	SSSS with Metal Scrap	25000	10	200	190	131
2	SSSS with Electric Heaters	26500	50	200	150	176
3	SSSS with Convection Heat Systems	25500	20	200	180	141

7. Future Scope

Future research will examine the efficiency of single-slope solar power while still utilizing alternative metal scraps, including steel and aluminum, as heat exchangers and considering variations in the mass and size of the metal scrap to enhance thermal performance. The evaluation will focus on the influence of environmental conditions, such as ambient humidity, seasonal variations, and geographic differences, to ensure system adaptability and long-term efficiency. Furthermore, operational parameters, including the absorber's surface area, glass cover angle, and basin water depth, will be examined to enhance performance. The study will examine the integration of advanced heat enhancement techniques, such as nanomaterials (CuO, Al_2O_3, and TiO_2) and phase change materials (PCMs), alongside hybrid systems that combine metal scrap with nanofluid-based absorbers or PCM-nanomaterial composites, to enhance heat retention and evaporation rates.

Conclusion

This research evaluates the performance of a single-slope solar still (SSSS) both with and without the incorporation of metal scrap heat enhancers. The study employs a Taguchi design of experiments, concentrating on key variables, including wind velocity (WV), water intake temperature (WI), and solar intensity (SI).

- The solar still basin is made of galvanized iron and finished in matte black. It is situated within a wooden shell lined with white to improve insulation and enhance solar absorption. The experiments conducted in Erode (latitude 11.3410° N, longitude 77.7172° E) considered water inlet temperatures (WI) ranging from 60 to 70°C, wind velocities (WV) between 1 and 5 m/s, and solar irradiance (SI) levels from 600 to 900 W/m², utilizing a tilt angle of 10°.
- The results indicate that productivity can attain a peak of 4.71 kg/m² under 900 W/m² solar irradiation, a water input temperature of 70°C, and a wind velocity of 3 m/s, highlighting the substantial impact of solar irradiation on system performance. WI exhibits a moderate effect, attaining peak performance at 65°C. In contrast, WV demonstrates a non-linear relationship, where moderate airflow enhances productivity, whereas excessive speeds reduce thermal efficiency.

- Analysis of variance (ANOVA) indicates that the most substantial contributor to variation is SI, which is the primary factor influencing production, followed by WI and WV. Regression equations indicate that increased SI and moderate WI positively impact productivity, T_w, and T_g, while WV shows minimal influence, except at high speeds.
- Interaction plots and contour analyses confirm these trends, indicating optimal system performance at high SI, moderate WI, and low-to-moderate WV. Contour plots demonstrate the combined effects of parameters, showing increased productivity and thermal stability at optimal configurations.

This study emphasizes the importance of adjusting input parameters to improve the efficiency of solar stills, thereby advancing the broader goal of developing sustainable water desalination techniques.

References

1. Shalaby, S. M., Hammad, F. A., & Zayed, M. E. (2023). Current progress in integrated solar desalination systems: Prospects from coupling configurations to energy conversion and desalination processes. Process Safety and Environmental Protection, 178, 494–510. https://doi.org/10.1016/j.psep.2023.08.058
2. Mahmoud, A., Fath, H., Ookwara, S., & Ahmed, M. (2019). Influence of partial solar energy storage and solar concentration ratio on the productivity of integrated solar still/humidification-dehumidification desalination systems. Desalination, 467, 29–42. https://doi.org/10.1016/j.desal.2019.04.033
3. Elashmawy, M., Ahmed, M. M. Z., Alawee, W. H., Shanmugan, S., & Omara, Z. M. (2024). Scientometric analysis and review of materials affecting solar still performance. Results in Engineering, 23, 102574. https://doi.org/10.1016/j.rineng.2024.102574
4. Demir, M. E., & Dincer, I. (2022). An integrated solar energy, wastewater treatment and desalination plant for hydrogen and freshwater production. Energy Conversion and Management, 267, 115894. https://doi.org/10.1016/j.enconman.2022.115894
5. Jayathunga, D. S., Karunathilake, H. P., Narayana, M., & Witharana, S. (2024). Phase change material (PCM) candidates for latent heat thermal energy storage (LHTES) in concentrated solar power (CSP) based thermal

applications - A review. Renewable and Sustainable Energy Reviews, 189, 113904. https://doi.org/10.1016/j.rser.2023.113904

6. Abed, A. F., Alshukri, M. J., & Hachim, D. M. (2024). Improving solar still performance via the integration of nanoparticle-enhanced phase change materials: A novel pyramid-shaped design with a numerical simulation approach. Journal of Energy Storage, 97, 112980. https://doi.org/10.1016/j.est.2024.112980
7. Jamil, F., Hassan, F., Shoeibi, S., & Khiadani, M. (2023). Application of advanced energy storage materials in direct solar desalination: A state of art review. Renewable and Sustainable Energy Reviews, 186, 113663. https://doi.org/10.1016/j.rser.2023.113663
8. Gajbhiye, T. S., Waghmare, S. N., Sirsat, P. M., Borkar, P., & Awatade, S. M. (2023). Role of nanomaterials on solar desalination systems: A review. Materials Today: Proceedings. https://doi.org/10.1016/j.matpr.2023.04.532
9. Singh, V. K., & Kumar, D. (2024). An experimental investigation and thermo-economic performance analysis of solar desalination system by using nano-enhanced PCM. Materials Today Sustainability, 27, 100884. https://doi.org/10.1016/j.mtsust.2024.100884
10. El Hadi Attia, M., Kabeel, A. E., Abdelgaied, M., & Abdel-Aziz, M. M. (2024). Experimental assessment of optimized size of sandstones as inexpensive natural thermal storage materials to improving the performance of hemispherical solar distillers. Environment, Development and Sustainability. https://doi.org/10.1007/s10668-024-04808-x
11. Dubey, A., & Arora, A. (2024). Effect of various energy storage phase change materials (PCMs) and nano-enhanced PCMs on the performance of solar stills: A review. Journal of Energy Storage, 97, 112938. https://doi.org/10.1016/j.est.2024.112938
12. Aly, W. I. A., Tolba, M. A., & Abdelmagied, M. (2023). Experimental investigation and performance evaluation of an oval tubular solar still with phase change material. Applied Thermal Engineering, 221, 119628. https://doi.org/10.1016/j.applthermaleng.2022.119628
13. Xu, B., Zhao, X., Zuo, X., & Yang, H. (2024). Progress of phase change materials in solar water desalination system: A review. Solar Energy Materials and Solar Cells, 271, 112874. https://doi.org/10.1016/j.solmat.2024.112874

14. Sharma, P., & Kumar Birla, S. (2024). Improving solar still efficiency with nanoparticles – Infused copper cylinders and latent heat storage: An experimental and simulation study. Applied Thermal Engineering, 243, 122650. https://doi.org/10.1016/j.applthermaleng.2024.122650
15. Selimefendigil, F., Şirin, C., & Öztop, H. F. (2022). Experimental analysis of combined utilization of CuO nanoparticles in latent heat storage unit and absorber coating in a single-slope solar desalination system. Solar Energy, 233, 278–286. https://doi.org/10.1016/j.solener.2022.01.039
16. krupakaran, R. L., Palampalle, B., Balasubramanian, D., & Reddy, G. V. (2020). Influence of Titanium Oxide Nanoparticle on Solar Desalination with Phase Change Material. SAE Technical Paper Series. https://doi.org/10.4271/2020-28-0464
17. Sonker, V. K., Singh, R. K., Chakraborty, J. P., & Sarkar, A. (2020). Performance assessment of a passive solar still integrated with thermal energy storage and nanoparticle stored in copper cylinders. International Journal of Energy Research, 45(2), 2856–2869. Portico. https://doi.org/10.1002/er.5982
18. Sharma, H. K., Kumar, S., Kumar, S., & Verma, S. K. (2022). Performance investigation of flat plate solar collector with nanoparticle enhanced integrated thermal energy storage system. Journal of Energy Storage, 55, 105681. https://doi.org/10.1016/j.est.2022.105681
19. Motahar, S., Alemrajabi, A. A., & Khodabandeh, R. (2017). Experimental study on solidification process of a phase change material containing TiO 2 nanoparticles for thermal energy storage. Energy Conversion and Management, 138, 162–170. https://doi.org/10.1016/j.enconman.2017.01.051
20. Mousa, H., Naser, J., Gujarathi, A. M., & Al-Sawafi, S. (2019). Experimental study and analysis of solar still desalination using phase change materials. Journal of Energy Storage, 26, 100959. https://doi.org/10.1016/j.est.2019.100959
21. Sonker, V. K., Chakraborty, J. P., & Sarkar, A. (2022). Development of a frugal solar still using phase change material and nanoparticles integrated with commercialization through a novel economic model. Journal of Energy Storage, 51, 104569. https://doi.org/10.1016/j.est.2022.104569

22. Yuvaperiyasamy, M., Senthilkumar, N., & Deepanraj, B. (2024). Application of nano materials in solar desalination system – a review. AIP Conference Proceedings. https://doi.org/10.1063/5.0196112
23. Javad Raji Asadabadi, M., & Sheikholeslami, M. (2022). Impact of utilizing hollow copper circular fins and glass wool insulation on the performance enhancement of pyramid solar still unit: An experimental approach. Solar Energy, 241, 564–575. https://doi.org/10.1016/j.solener.2022.06.029
24. Yuvaperiyasamy, M., Senthilkumar, N., & Deepanraj, B. (2024). Enhancing Pyramid Solar Still Performance through Varied Heat Storage Materials and Water Depths: A Comprehensive Experimental Study. Recent Patents on Mechanical Engineering, 17. https://doi.org/10.2174/0122127976288061240228045000
25. Yuvaperiyasamy, M., Senthilkumar, N., & Deepanraj, B. (2023). Experimental investigation on the performance of a pyramid solar still for varying water depth, contaminated water temperature, and addition of circular fins. International Journal of Renewable Energy Development, 12(6), 1123–1130. https://doi.org/10.14710/ijred.2023.57327
26. Wang, J., Xie, H., Guo, Z., Guan, L., & Li, Y. (2014). Improved thermal properties of paraffin wax by the addition of TiO2 nanoparticles. Applied Thermal Engineering, 73(2), 1541–1547. https://doi.org/10.1016/j.applthermaleng.2014.05.078
27. Samara, H., Hamdan, M., & Al-Oran, O. (2024). Effect of Al2O3 nanoparticles addition on the thermal characteristics of paraffin wax. International Journal of Thermofluids, 22, 100623. https://doi.org/10.1016/j.ijft.2024.100623
28. Ali, A. H., Ibrahim, S. I., Jawad, Q. A., Jawad, R. S., & Chaichan, M. T. (2019). Effect of nanomaterial addition on the thermophysical properties of Iraqi paraffin wax. Case Studies in Thermal Engineering, 15, 100537. https://doi.org/10.1016/j.csite.2019.100537
29. Bharathiraja, R., Ramkumar, T., & Selvakumar, M. (2023). Studies on the thermal characteristics of nano-enhanced paraffin wax phase change material (PCM) for thermal storage applications. Journal of Energy Storage, 73, 109216. https://doi.org/10.1016/j.est.2023.109216

30. Nabwey, H. A., & Tony, M. A. (2023). Thermal Energy Storage Using a Hybrid Composite Based on Technical-Grade Paraffin-AP25 Wax as a Phase Change Material. Nanomaterials, 13(19), 2635. https://doi.org/10.3390/nano13192635
31. Praveen, N., Mallik, U. S., Shivasiddaramaiah, A. G., Hosalli, R., Prasad, C. D., & Bavan, S. (2024). Machinability Study of Cu-Al-Mn Shape Memory Alloys using Taguchi Method. Journal of The Institution of Engineers (India): Series D. https://doi.org/10.1007/s40033-023-00629-w
32. Awd Allah, M. M., Abd El Aal, M. I., & Abd El-baky, M. A. (2024). Optimizing the crashworthy behaviors of hybrid composite structures through Taguchi approach. Polymer Composites, 45(9), 7906–7917. Portico. https://doi.org/10.1002/pc.28312
33. El-Sebaii, A. A. (2011). On effect of wind speed on passive solar still performance based on inner/outer surface temperatures of the glass cover. Energy, 36(8), 4943–4949. https://doi.org/10.1016/j.energy.2011.05.038
34. Nagaraja, B., Almeida, F., Yousef, A., Kumar, P., Ajaykumar, A. R., & Al-Mdallal, Q. (2023). Empirical study for Nusselt number optimization for the flow using ANOVA and Taguchi method. Case Studies in Thermal Engineering, 50, 103505. https://doi.org/10.1016/j.csite.2023.103505
35. Gnanaraj, S. J. P., & Ramachandran, S. (2017). Optimization on performance of single-slope solar still linked solar pond via Taguchi method. DESALINATION AND WATER TREATMENT, 80, 27–40. https://doi.org/10.5004/dwt.2017.20583
36. Subramanian, K., Meenakshisundaram, N., & Barmavatu, P. (2024). Experimental and theoretical investigation to optimize the performance of solar still. Desalination and Water Treatment, 318, 100343. https://doi.org/10.1016/j.dwt.2024.100343
37. Dhivagar, R., Mohanraj, M., Hidouri, K., & Midhun, M. (2021). CFD modeling of a gravel coarse aggregate sensible heat storage assisted single slope solar still. Desalination and water treatment, 210, 54–69. https://doi.org/10.5004/dwt.2021.26554
38. Uslu, S., & Aydın, M. (2020). Effect of operating parameters on performance and emissions of a diesel engine fueled with ternary blends of palm oil biodiesel/diethyl ether/diesel by Taguchi method. Fuel, 275, 117978. https://doi.org/10.1016/j.fuel.2020.117978

39. Chen, W.-H., Carrera Uribe, M., Kwon, E. E., Lin, K.-Y. A., Park, Y.-K., Ding, L., & Saw, L. H. (2022). A comprehensive review of thermoelectric generation optimization by statistical approach: Taguchi method, analysis of variance (ANOVA), and response surface methodology (RSM). Renewable and Sustainable Energy Reviews, 169, 112917. https://doi.org/10.1016/j.rser.2022.112917
40. Yuvaperiyasamy, M., Senthilkumar, N., & Deepanraj, B. (2023). Experimental and theoretical analysis of solar still with solar pond for enhancing the performance of sea water desalination. Water Reuse, 13(4), 620–633. https://doi.org/10.2166/wrd.2023.102
41. Tony, M. A., & Nabwey, H. A. (2024). Recent advances in solar still technology for solar water desalination. Applied Water Science, 14(7). https://doi.org/10.1007/s13201-024-02188-1
42. Nagaraju, V., Murali, G., Bewoor, A. K., Kumar, R., Sharifpur, M., Assad, M. E. H., & Awad, M. M. (2022). Experimental study on performance of single slope solar still integrated with sand troughs. Sustainable Energy Technologies and Assessments, 50, 101884. https://doi.org/10.1016/j.seta.2021.101884
43. Tamizharasan, T., Senthilkumar, N., Selvakumar, V., & Dinesh, S. (2019). Taguchi's methodology of optimizing turning parameters over chip thickness ratio in machining P/M AMMC. SN Applied Sciences, 1(2). https://doi.org/10.1007/s42452-019-0170-8